Earthquake sensitivity to tides and seasons: theoretical studies

François Pétrélis, Kristel Chanard, Alexandre Schubnel, Takahiro Hatano

Earthquake sensitivity to tides and seasons: theoretical studies

François Pétrélis,[1] Kristel Chanard,[2] Alexandre Schubnel,[3] and Takahiro Hatano[4]

[1]*Laboratoire de Physique Statistique, Ecole Normale Supérieure, PSL Research University, Université Paris Diderot Sorbonne Paris-Cité, Sorbonne Universités UPMC, Univ Paris 06, and CNRS, 24 rue Lhomond, 75005 Paris, France*

[2]*Université de Paris, Institut de physique du globe de Paris, CNRS, IGN, F-75005 Paris, France*

[3]*Laboratoire de Géologie, CNRS UMR 8538, Ecole normale Supérieure, PSL Research University, Paris, France*

[4]*Department of Earth and Space Science, Osaka University, 560-0043 Osaka, Japan*

Abstract

We investigate theoretically the effects of periodic-in-time modulations on the properties of earthquakes. To wit, we consider successively the one dimensional Burridge-Knopoff (BK) model and the two dimensional Olami-Feder-Christensen (OFC) model. Each model is modified to take into account either a modulation of normal stress or of shear stress acting on a fault. Despite the differences between the BK and the OFC model, several results are observed in both models. In particular, we observe that earthquake occurrences correlate with stress modulation. The correlation is strongly dependent on parameters such as the type of modulation, its frequency and amplitude, and in some cases on the magnitude of the considered earthquakes.

PACS numbers:

In the Earth's crust, at seismogenic depths, transient changes in stress can be caused by various sources. As such, the possibility that tides have an influence on earthquakes has been debated for more than a century among seismologists [1]. Even though tidal stress modulations are small compared to those of fault dynamics, they occur on a short timescale so that properties sensitive to variation rates could be affected by tides. Models based on Rate and State (R & S) friction laws [2] proposed that short-period stress transients are not effective at triggering earthquakes if they occur faster than the characteristic earthquake nucleation duration. Similar R & S models were used, later on, to explain the poor correlation between tidal loading and earthquakes [3].

However, several robust studies showed a statistically significant correlation between earthquakes and oceanic or solid Earth tides [4–7], and even at higher frequencies between dynamic triggering from seismic waves and earthquakes [8]. Recent studies have also shown that the fraction of large earthquakes increases when the tidal stress increases [9]. This effect depends on the faulting geometry and correlation with the shear stress was only observed for reverse faulting [10]. The correlation with tides has also been reported to have increased prior to several large earthquakes and to have disappeared afterwards [11, 12].

Similarly, seasonal effects such as snow or water loadings are also possible sources of modulation on faults. It has been reported that deep-focus earthquakes (magnitude larger than 7, depth larger than 500 km) are two to three times more likely in summer [13]. Similarly, it has been reported that the annual variation of terrestrial water mass is a possible source of modulation of seismicity on faults in different tectonic settings such as the Himalayas of Nepal [14, 15], California [16, 17], in the New Madrid region [18] or in the Southwest of Japan [19].

Despite these numerous observations, only a few theoretical studies have considered this problem. Considering one degree of freedom subject to periodic shear stress modulation, it was shown that the earthquake rate is proportional to the frequency of the modulation [20]. Here we consider two discrete models of fault with many degrees of freedom so that the size-dependent properties (including the Gutenberg-Richter law) are investigated. A different approach would have been to adopt a continuum model, but it generally fails to reproduce the GR law [21] and therefore does not fit our purpose. For each of the two models, we investigate the properties of the earthquakes when either normal stress or shear stress on a fault is modulated periodically in time. Our results provide a quantitative explanation of the sensitivity to periodic loading of earthquake statistical properties including the size distribution.

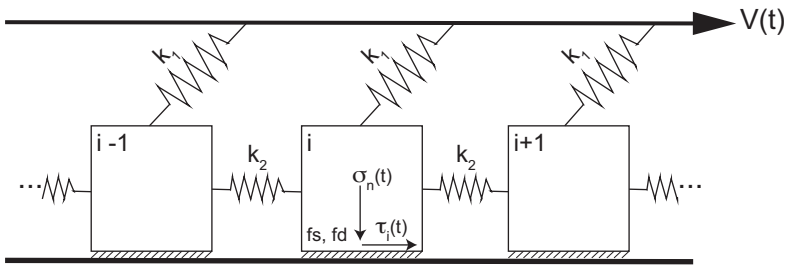

FIG. 1: Schematics of the model. The i-th block is pushed by its neighbours and the moving plate of speed $V(t)$.

ONE DIMENSIONAL BURRIDGE-KNOPOFF MODEL

Description of the models

Our first analysis on the effect of stress modulation on earthquakes is based on the one-dimensional Burridge-Knopoff (BK) model shown in Fig. 1, where a set of N sliders are located on a line at positions $\hat{x}_i$. Each slider is connected to its nearest neighbours with a spring of stiffness $\hat{k}_2$. The first and the last sliders are only connected to one neighbour. In addition, each slider is connected with a spring of stiffness $\hat{k}_1$ to a plate that moves at constant velocity denoted by $\hat{v}_0$. To make contact between this model and a continuum, these sliders should be interpreted as the elements of unit surface that constitute the fault. Thus, forces and stresses have the same dimension in our model.

The driving force on the i-th slider is

$$\hat{\tau}_i = -\hat{k}_2(2\hat{x}_i - \hat{x}_{i+1} - \hat{x}_{i-1}) + \hat{k}_1(\hat{v}_0\hat{t} - \hat{x}_i)\,. \tag{1}$$

If this driving force $\hat{\tau}_i$ reaches the static friction force $\hat{F}_s$ at slider i, it starts to move with velocity $\hat{v}_i$ and is subject to the dynamic friction force

$$\hat{F}_d(\hat{v}_i) = \hat{F}\frac{1-\delta}{1+\frac{2\hat{\alpha}}{1-\delta}\hat{v}_i} \tag{2}$$

where δ and $\hat{\alpha}$ are positive constants. δ corresponds to the instantaneous stress drop from static friction to dynamic friction. Note also that the dynamic friction decreases as the slip velocity $\hat{v}_i$ increases. Such friction is referred to as the velocity weakening friction, and $\hat{\alpha}$ represents the amplitude of the negative velocity dependence. Then we are led to the equation of motion for

slider i [22]:

$$\frac{d}{dt}\hat{v}_i = \hat{\tau}_i - \hat{F}_d(\hat{v}_i). \tag{3}$$

In addition, each slider is not allowed to move backward and if its velocity vanishes with a negative acceleration, it is set to zero.

Using the BK model described above, we analyze the effect of stress modulation on earthquake occurrence. In natural earthquake faults, the stress modulation may affect both normal and shear stresses, the amplitude of which depends on the faulting orientation. For instance, on strike-slip faults, which dip vertically, normal stress is not much modulated, whereas reverse faults, with lower dip angle, may be subject to relatively large modulation in normal stress. Taking these geometrical effects into account, here we consider two extreme models: the normal stress modulation (NSM) model and the shear stress modulation (SSM) model.

In the NSM model, the normal stress is modulated while the shear stress is constant. In the equation, the normal stress modulation results in a modulated friction force. Thus, the static friction reads

$$\hat{F}_s = \hat{F}(1 + \varepsilon \cos \hat{\Omega}\hat{t}), \tag{4}$$

where ε is the amplitude of modulation and $\hat{\Omega}$ is the frequency. Similarly, the dynamic friction is obtained by replacing $\hat{F}$ with $\hat{F}(1 + \varepsilon \cos \hat{\Omega}\hat{t})$ in Eq. (2).

The second (SSM) model consists in a modulation of the shear stress. More precisely, we assume the additional driving force $-\hat{F}\varepsilon \cos \hat{\Omega}\hat{t}$ in Eq. (1). This may result either from the periodic stressing or from the modulation of plate velocity. As the normal stress is kept constant here, the static and dynamic friction forces are also constants: *i.e.*, we set $\varepsilon = 0$ in Eqs. (2) and (4). With these definitions, the condition to initiate an EQ is the same as for the NSM model, whereas the dynamical equation is different. Importantly, the dynamic friction is independent of the modulation phase (the value of $\hat{\Omega}\hat{t}$) in the SSM model.

For the parameters that we consider here, the events during which sliders are moving occur on a very short time scale compared to $\hat{F}/(\hat{k}_1 \hat{v}_0)$ and $1/\hat{\Omega}$ so that the time dependent term of the dynamic friction ($\varepsilon \cos \hat{\Omega}\hat{t}$) and the position of the moving plate are set fixed to their values at the beginning of the motion.

In both models, using $1/\sqrt{\hat{k}_1}$ as unit of time and $\hat{F}/\hat{k}_1$ as unit of length, we can set $\hat{k}_1$ and $\hat{F}$ to unity. In other words, we write $\hat{k}_2 = \hat{k}_1 K$, $\hat{v}_0 = v_0 \hat{F}/\sqrt{\hat{k}_1}$, $\hat{\alpha} = \alpha\sqrt{\hat{k}_1}/\hat{F}$ and change variables using $\hat{x} = x\hat{F}/\hat{k}_1$ and $\hat{t} = t/\sqrt{\hat{k}_1}$. Then the equations for $x(t)$ involve only $K = \hat{k}_2/\hat{k}_1$, $v_0 = \hat{v}_0\sqrt{\hat{k}_1}/\hat{F}$

and $\alpha = \hat{\alpha}\hat{F}/\sqrt{\hat{k}_1}$. There are thus seven dimensionless control parameters: N, δ, K, v_0, α, ε, and $\Omega = \hat{\Omega}/\sqrt{\hat{k}_1}$.

Results

No modulation

Unless otherwise stated, we use $\delta = 0.01$, $N = 800$, $\alpha = 1$, $v_0 = 10^{-8}$, and $K = 9$ [23]. For these parameters, the system alternates between a loading period in which the sliders are at rest and the driving force τ_i increases linearly in time and a brief event initiated once one of the sliders starts moving and can put into motion a varying number of sliders. These sudden events are interpreted as the earthquakes (EQ) in the BK model. The system has a chaotic behavior and in particular the size of the EQ fluctuates. The released energy during an EQ is characterized by the magnitude M defined as $M = \log(\sum_i \Delta x_i)$, where Δx_i is the distance over which each slider has moved during an event. For the parameters chosen here and in absence of modulation, the distribution of M is an exponential, reminiscent of the Gutenberg-Richter (GR) law. Writing $P(M) = 10^{-bM_s}$ where $M_s = \frac{2}{3}\log(\sum_i \Delta x_i)/\log(10)$, the value of b ranges between $3/4$ and 1 and its exact value depends on the range of magnitude over which is it estimated.

Natural earthquakes display the GR law. To observe this law in the BK model, most of the parameters have to be either large or small. In particular N is large to consider a large system, v_0 is very small to have separated time scales between loading and events, and the stress drop δ is small. The results will not be drastically changed if we increase further N or decrease v_0 or δ. In other words, we are in the limit of large N and small v_0 and δ and no qualitative change will occur if we modify their values.

Modulated normal stress (NSM) model

We start with a description of the results obtained with the NSM model. We have varied Ω between 10^{-8} and 10^{-3}. Compared to the mean interevent time $T \simeq 3.3 \times 10^4$ in absence of modulation, or to the mean duration between motion of a given block which we estimate of order $NT \simeq 2 \times 10^7$ or smaller, we span both regimes of fast and slow force modulation $3.3 \times 10^{-4} \leq$

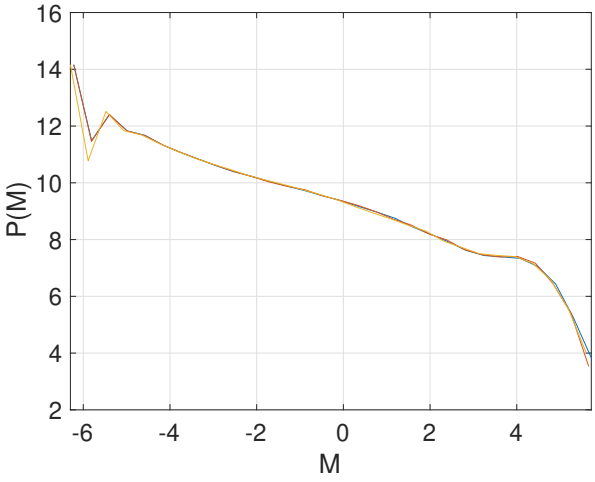

FIG. 2: Probability density function (PDF) of magnitude M, for $\varepsilon = 0$; $\Omega = 10^{-7}$, $\varepsilon = 0.03$ and $\Omega = 10^{-3}$, $\varepsilon = 5\,10^{-6}$. The three curves are nearly superimposed.

$\Omega T \leq 33$ and $0.2 \leq \Omega N T \leq 2 \times 10^4$.

Amongst the most important properties of the solutions of the BK model are the statistical distributions of the inter-event time T between two consecutive earthquakes and of the earthquake magnitudes. As will be discussed later, the behavior of the system drastically changes for large values of the modulation amplitude [24]. Otherwise, we observe that the mean inter-event time T, its rms fluctuations and its distribution are independent of ε. Similarly, the magnitude distribution remains unchanged, as can be seen in fig. 2. Stated differently, the modulation of the friction force has no effect on these properties. Nevertheless, the system is affected by the modulation. As displayed in fig. 3, the event rate $\frac{dn}{dt}$ varies with time with a period equal to that of the force modulation.

To quantify this effect, we calculate for each event, its phase Φ defined as Ωt_e modulo 2π where t_e is the time at which an event occurs. We then calculate the probability density function (PDF) of the phase $P[\Phi]$, which is displayed in fig. 4.

We observe that the PDF is an harmonic function and is well fitted by $\frac{1}{2\pi} + a\sin(\Phi - \Delta\Phi)$ (black curves in the figures). The amplitude a and the phase shift $\Delta\Phi$ of the PDF's harmonic response characterize the sensitivity of the system to the force modulation. The amplitude a is an increasing function of ε and Ω as shown in fig. 5.

We calculate the value $\varepsilon_c(\Omega)$ at which a reaches an arbitrary small value taken to be $a_c = \sqrt{2} \times$

10^{-2} (fig. 6) and observe two behaviors: at large Ω it satisfies $\varepsilon_c \simeq 8.2 \times 10^{-10}/\Omega$, and at smaller Ω it crossovers to a constant value or to less steep behavior at least. The crossover frequency is of the order of $\Omega_c = 10^{-6}$. The results for a are collapsed if displayed as a function of $\varepsilon/\varepsilon_c$ (fig. 7). For moderate values of $\varepsilon/\varepsilon_c$, a linear behavior is observed of the form $a \simeq 1.36 \times 10^{-2}\varepsilon/\varepsilon_c$.

We note that for ε larger than roughly $10\,\varepsilon_c$, $P[\Phi]$ vanishes for a given range of Φ, meaning moments of quiescence in the system. More precisely, for very large ε, events occur only when the friction force is the smallest. In that situation, some properties of the system change. In particular, the distribution of the inter-event time displays peaks for values equal to multiples of the force period. As a consequence, the mean and the standard deviation of the interevent time start to depend on ε. In this regime, the effect of the modulation is very strong. In particular, it leads to the absence of events for certain values of the phase. Because such properties have not been observed (yet) by observational seismology, we focus on smaller values of the modulation, $\varepsilon \leq 10\,\varepsilon_c$.

For large enough Ω and small ε, using the expression for ε_c, we obtain $a \simeq 1.6 \times 10^7\,\varepsilon\Omega$ which can be written as $av_0/(\varepsilon\Omega) \simeq 0.16$. Using the dimensionless parameters, we expect a relation of the form

$$a = \Pi(N, \delta, K, v_0, \alpha, \varepsilon, \Omega) \tag{5}$$

where Π is an unknown function. Having observed that a is linear in ε, we write this expression as

$$a = \varepsilon\Omega/v_0\; h(N, \delta, K, v_0, \alpha, \Omega)\,. \tag{6}$$

For large Ω, the unknown function $h = av_0/(\varepsilon\Omega)$ is thus independent of Ω and takes the value 0.16. We have checked that the same value is obtained for $\Omega = 10^{-2}$ and $v_0 = 10^{-7}$, so that for this range of parameters, h depends neither on v_0 nor on Ω.

We have investigated the dependence of $h = av_0/(\varepsilon\Omega)$ on some of the other parameters by changing Ω, α and N. The effects of the frequency and of the number of sliders are displayed in fig. 8. As mentioned, for large Ω, h is a constant. It increases when Ω becomes smaller. The variation with Ω is reduced when the number of sliders is decreased. In addition for large Ω, reducing the number of sliders by a factor up to 4 leaves the value of h nearly unchanged.

The effect of the proximity to criticality is investigated by changing α. Indeed $\alpha = 1$ corresponds to the regime in which the GR law is observed for the widest range of magnitudes. When α is large, a peak of events appears for large magnitudes which is reminiscent of characteristic

earthquakes. As for small α, the largest events are less frequent which corresponds to an increase in the b-value [25]. For $1/2 \leq \alpha \leq 1$, our results show that h is constant (fig. 8), and thus independent of the b-value within this range. In contrast, h is decreased at larger α, *i.e.* by the existence of characteristic events.

Having discussed the properties of a, we now discuss those of the phase-shift $\Delta\Phi$ between $-\frac{dF_r}{dt}$ and $P[\Phi]$ as a function of Ω (fig. 9). Its value is roughly independent of ε in the vicinity of ε_c. We note that $\Delta\Phi$ is close to 0 apart for the small values of Ω where it increases. This corresponds to frequency Ω smaller than $\Omega_c \simeq 10^{-6}$.

The large Ω regime corresponds to $\Delta\Phi \simeq 0$, so that events are more frequent when the decay rate of the friction force is larger. Equivalently there are less events when the increase rate of the friction force is larger. For smaller Ω, the behavior is changed. It appears that $\Delta\Phi$ evolves towards $\pi/2$. Events are then more frequent when the friction force is the smallest.

The analysis of the phase of the events presented so far has been made taking into account all the events, independently of their magnitudes. To investigate how the triggering depends on the magnitude, we focus on two parameter values: large frequency $\Omega = 10^{-3}$ and small frequency $\Omega = 10^{-7}$. For values of ε slightly above ε_c, we have computed numerically very large set of events and calculated the distribution of the phase $P_{Ms}(\Phi)$ obtained when only events of magnitude larger than M_s are considered. For large Ω, the distribution of the phase $P_{Ms}(\Phi)$ is unchanged when we change M_s. In constrast for smaller Ω, we observe a change in the distribution of the phase of the events when M_s is changed (fig. 10).

Let us now detail properties observed at the small Ω. Considering all magnitudes, the events are more likely to occur for $\Delta\Phi$ between 0 (largest decay rate) and $\pi/2$ (force is the smallest). Increasing M_s, for intermediate magnitude, the modulation of the phase decreases so that the triggering is less visible. In contrast, if we consider only the very large magnitudes, we observe a clear modulation of the phase of the events: they are more frequent when the friction force is the largest. For $M_s = 5.75$ which corresponds to 2875 events over a total number of events of 1.15 billions of events, there are 1.3 times more events when the force is maximum than when it is minimum. Considering all the magnitudes, we observe the opposite: 1.22 times more events at the force minimum. This effect is also present at smaller values of ε, the amplitude of the modulations of the phase distribution being reduced.

A different way to analyze this property is to study the GR law as a function of the phase. The b-value calculated over intermediate values of M ($0.5 < M < 3$) varies with the phase (fig. 11).

Finally, we calculated the cumulative moment (here equal to the cumulative displacement $\sum \Delta X_i$), where the sum is taken over events of given phase (fig. 12). We note that the phase dependence of the cumulative moment is similar to the one of the PDF of the phase of the large events. This is expected for b-values lower than $3/2$. Indeed the Gutenberg-Richter law corresponds to a moment distributed as a power law with exponent $2b/3$. Considering such a distribution cutted off at low and large values, the average of the moment is dominated by the largest events if $b < 3/2$. In other words, when the b-value is smaller than $3/2$, large earthquakes dominate the moment release. In such way, here, the moment release depends on the phase of the modulation Φ, this property being true whether we consider all the events, or only those with $M \geq 0$ or $M \geq 4$.

We conclude the presentation of the results in this model by noting the non trivial differences in the behavior when limits are taken. For the large Ω limit, the behavior depends on how the limit is taken but does not depend on the magnitude of the considered events. At fixed ε, moments of quiescence are observed and events only occur when the normal stress is the smallest. At fixed and not too large $\varepsilon\Omega$, the response remains linear in $\varepsilon\Omega$ and events are more likely to occur when the stress decay rate is the largest. In the small Ω limit, event distributions depend on their magnitude. Largest events occur when the stress is the largest, smallest event occur when the stress is the smallest. The amplitude of the response is increasing with ε and linear for small ε.

Shear stress model

The results presented so far are obtained with a model that describes a modulated normal stress (NSM). We now turn to the case of a modulation of the shear stress (SSM). The results in both models are similar: EQ occur more often for given values of the phase. For moderate values of ε, the phase modulation is well fitted by a sin-function which amplitude is linear in ε. In this regime and for the range of parameters that we consider, we obtain nearly the same values of $h = av_0/(\varepsilon\Omega)$ for both models [32]. We observe a phase-shift close to $\Delta\phi = 0$ for all values of Ω. However, we do not observe for the SSM a variation of the pdf of the phase $P_{M_s}(\Phi)$ when we change M_s. Even considering the largest possible values of M_s, the modulation of $P_{M_s}(\Phi)$ remains the same as the one obtained when considering all events. This means that the sensitivity on magnitude of the phase-distribution of the EQ is strongly dependent on the nature of the modulation. It is not present when the shear stress is modulated, whereas it is clearly visible when the normal stress is modulated with a small frequency Ω.

THE TWO DIMENSIONAL OLAMI-FEDER-CHRISTENSEN MODEL

Description of the models

The second system that we consider is the Olami-Feder-Christensen (OFC) model [29]. The OFC model is a two-dimensional cellular automaton describing the evolution of N^2 degrees of freedom located on a square network. The dynamical variable F_i is called the stress.

Starting from an initial condition where all F_i are smaller than the maximum static friction force F_0, the system is at rest and a load increases the value of all the F_i until one of the degrees of freedom, say j reaches F_0. Then the value of F for all the neighbors of j is increased by the value of F_j multiplied by a coefficient α. Subsequently F_j is set to zero. If for one of the neighbors, F is larger than F_0, the process continues. It stops when all values of F_i are smaller than F_0.

These events are considered to be the earthquakes of the model. The magnitude of the event is the number of degrees of freedom that have have reached F_0. As the same degree of freedom can reach F_0 several times during the same event, the magnitude of the event can be larger than the number of degrees of freedom involved in the event.

Boundary conditions play a very important role for the OFC model. Here, sites at the border of the system follow the same dynamical rule as the ones in the bulk: they transfer $\alpha/4$ of their stress to their neighboors. Stress transferred outside of the system is lost. These standard boundary conditions are called open boundary conditions.

In general, temporal aspects of the OFC system are not considered, but see [30] for a study of foreshocks and aftershocks. Here we first assume that the loading of the system is performed at fixed velocity, i.e. the loading rate is constant so that during the load, all F_i are increased by a term $v_0 t$. In addition we consider that the events are very brief compared to $1/v_0$ so that the time does not evolve during the event. With these two assumptions, we can define a time of occurence to each event, say T.

Periodic modulation of the system is first introduced by assuming that F_0 is changed. This corresponds to the modulation of the normal stress (NSM model) as described for the BK model. Without loss of generality we thus consider that $F_0 = 1 + \varepsilon \cos(\Omega t)$.

We have considered a second model in which F_0 is fixed to 1 but the stress is modulated. In line with the studies on the BK model, this corresponds to a modulated shear stress model (SSM). We thus add a term $-\varepsilon \cos(\Omega t)$ to the stress F_i during the loading phases. In other words the stress

increases as $v_0 t - \varepsilon \cos(\Omega t)$ when the degrees of freedom are at rest. The negative sign is chosen so that the condition for initiation of an EQ is the same as when the friction force is modulated.

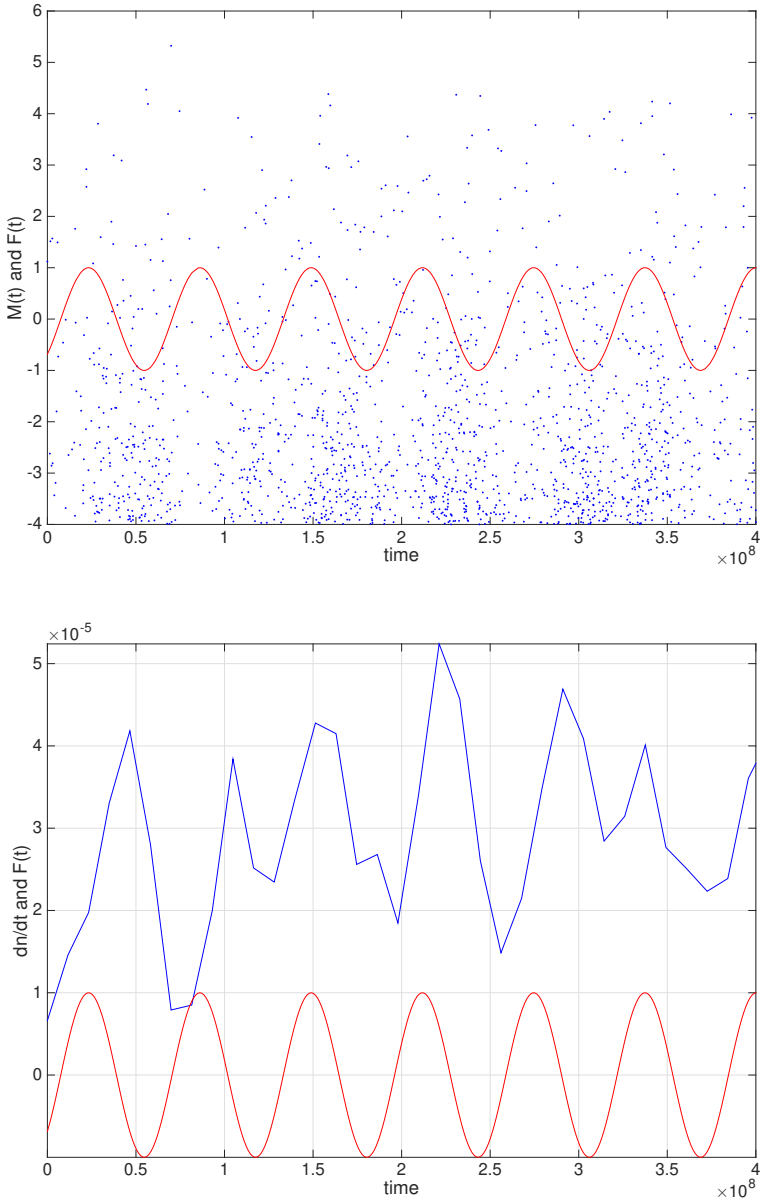

FIG. 3: Top: Magnitude (restricted to $M > -4$) of EQ as a function of time for $\varepsilon = 0.03$ and $\Omega = 10^{-7}$ (blue dots), the red curve is proportional to the modulated force. Bottom: occurence rate dn/dt of the EQ as a function of time (blue curve) for $\varepsilon = 0.03$ and $\Omega = 10^{-7}$, the red curve is proportional to the stress modulation.

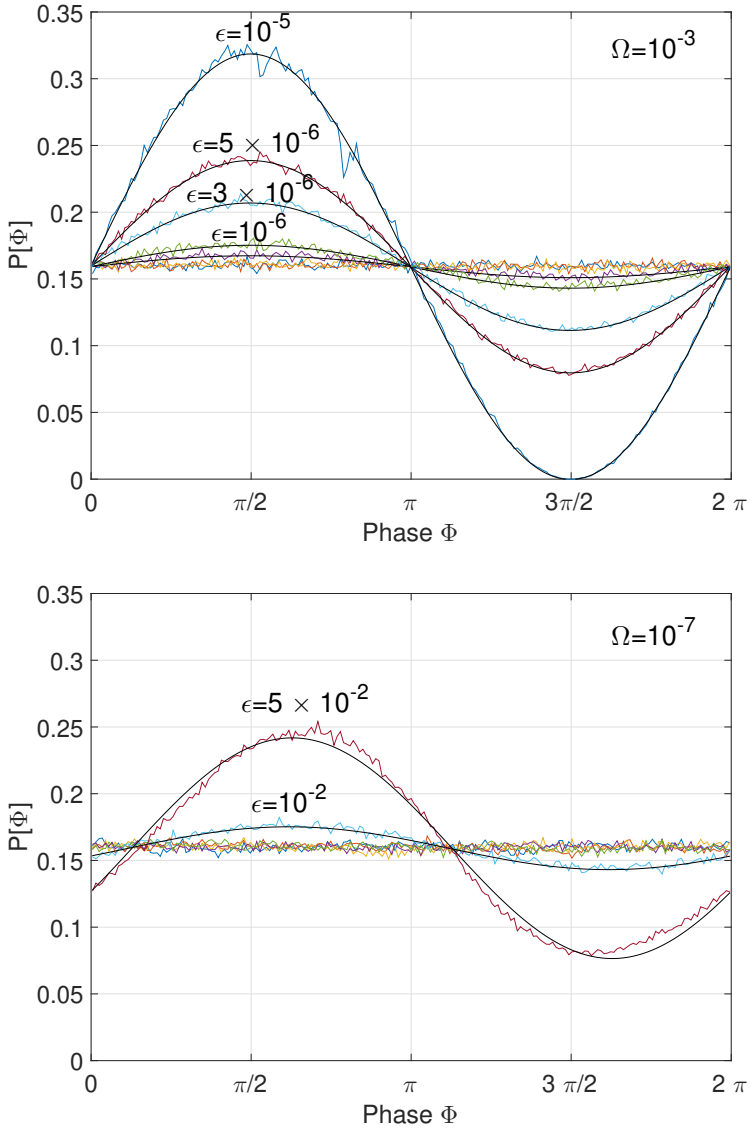

FIG. 4: Probability density function (PDF) $P[\Phi]$ for different ε and top: $\Omega = 10^{-3}$, dark blue $\varepsilon = 10^{-5}$, red 5×10^{-6}, light blue 3×10^{-6}, green 10^{-6}, magenta 5×10^{-7}, other curves are smaller ε. Bottom: $\Omega = 10^{-7}$, red: $\varepsilon = 0.05$, blue: $\varepsilon = 0.01$, other curves are smaller ε. Colored curves are the data and the black curves are the sin fits: $a\sin(\Phi - \Delta\Phi)$.

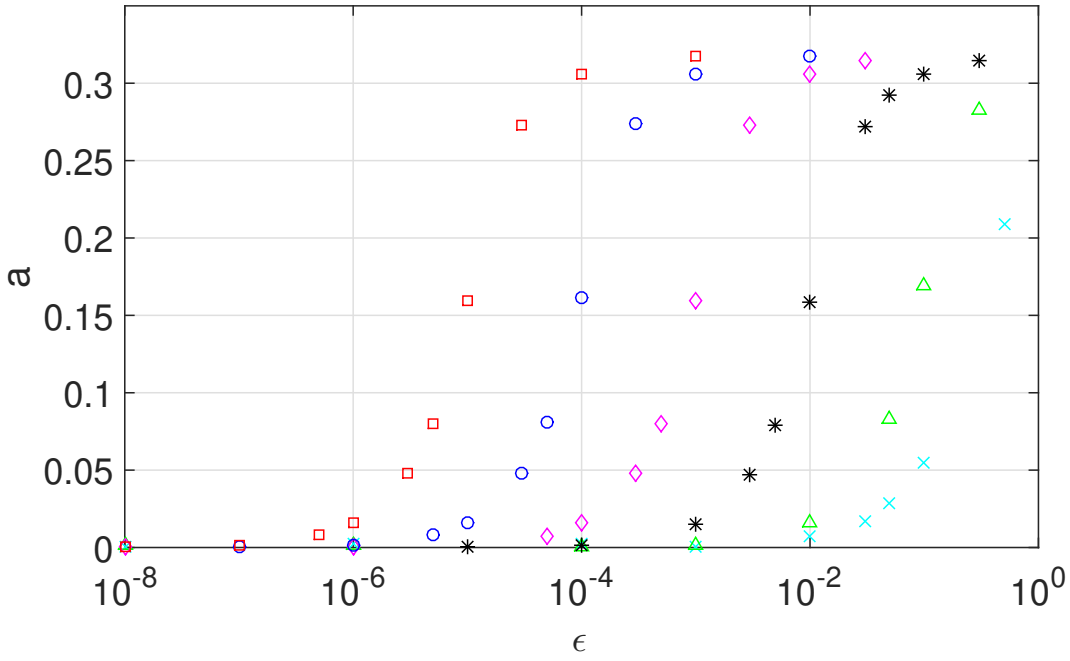

FIG. 5: Amplitude of the modulation of the phase distribution a as a function of ε for different frequencies, $\square$ red: $\Omega = 10^{-3}$; $\circ$ blue : $\Omega = 10^{-4}$; $\diamond$ magenta : $\Omega = 10^{-5}$; $\star$ black : $\Omega = 10^{-6}$; $\triangle$ green : $\Omega = 10^{-7}$; $\times$ cyan : $\Omega = 10^{-8}$.

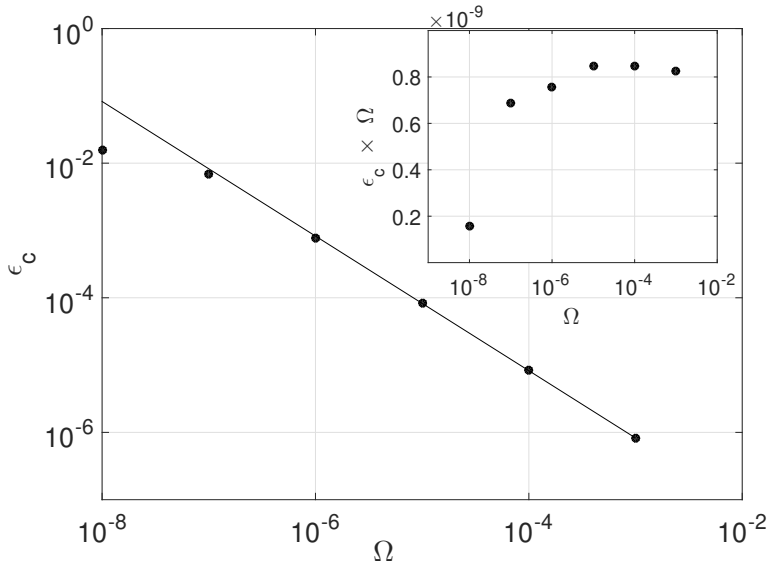

FIG. 6: ε_c as a function of Ω. Insert: $\Omega\,\varepsilon_c$ as a function of Ω.

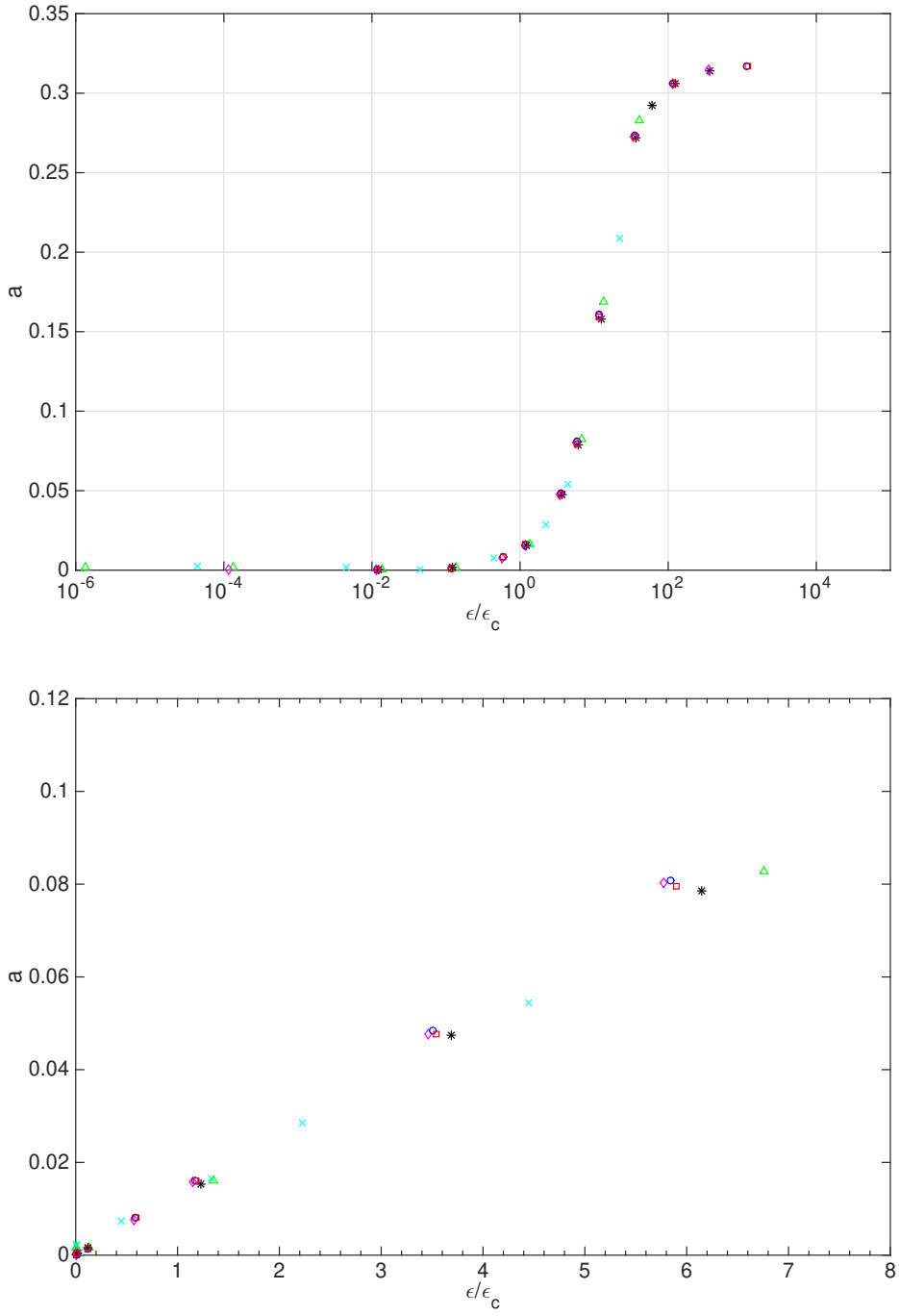

FIG. 7: Amplitude of the modulation of the phase distribution a as a function of $\varepsilon/\varepsilon_c$ for different frequencies, $\square$ red: $\Omega = 10^{-3}$; $\circ$ blue : $\Omega = 10^{-4}$; $\diamond$ magenta : $\Omega = 10^{-5}$; $\star$ black : $\Omega = 10^{-6}$; $\triangle$ green : $\Omega = 10^{-7}$; $\times$ cyan : $\Omega = 10^{-8}$. Bottom: zoom on the origin in lin-lin scale

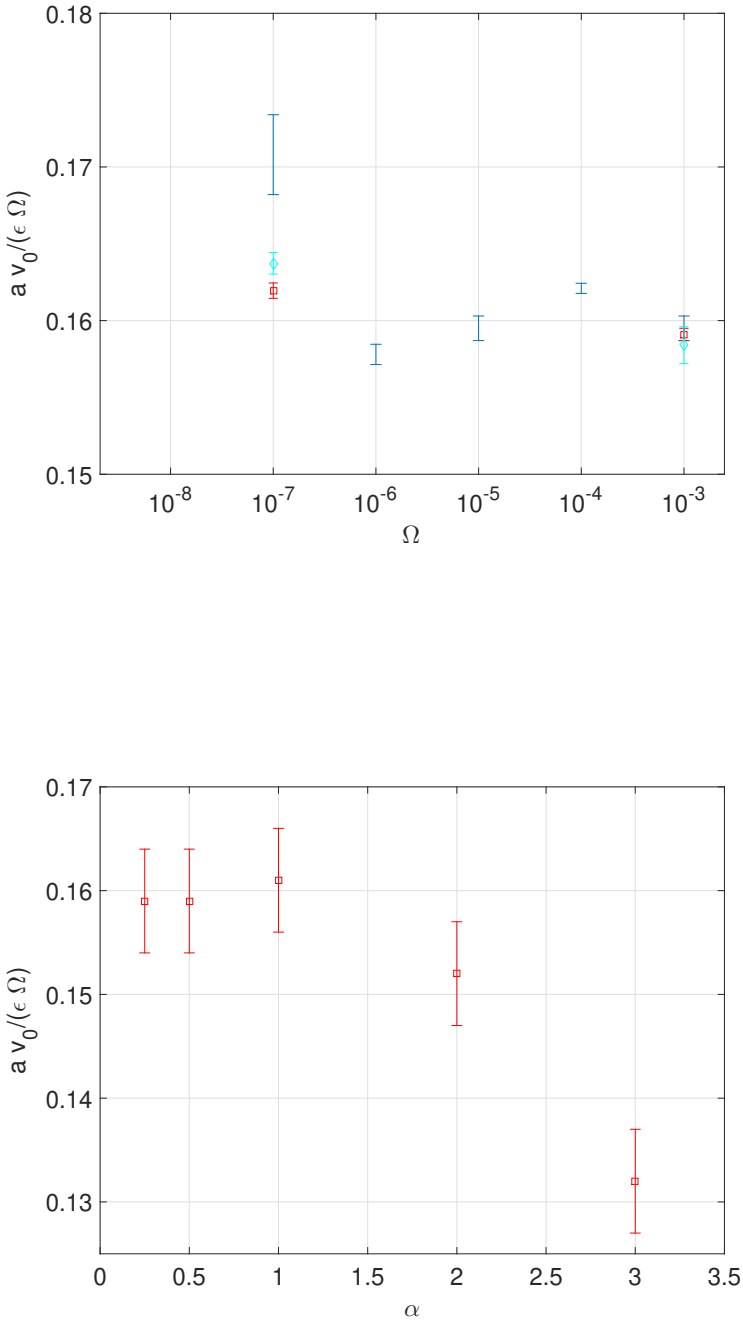

FIG. 8: $av_0/(\varepsilon\Omega)$ for small ε. Top: as a function of Ω. The value for $\Omega = 10^{-8}$ is 0.55, not displayed to focus on the smaller variations with N and at larger Ω. In blue $N = 800$, in cyan $N = 400$, in red $N = 100$. Bottom: as a function of α and for $\Omega = 10^{-3}$ and $N = 800$.

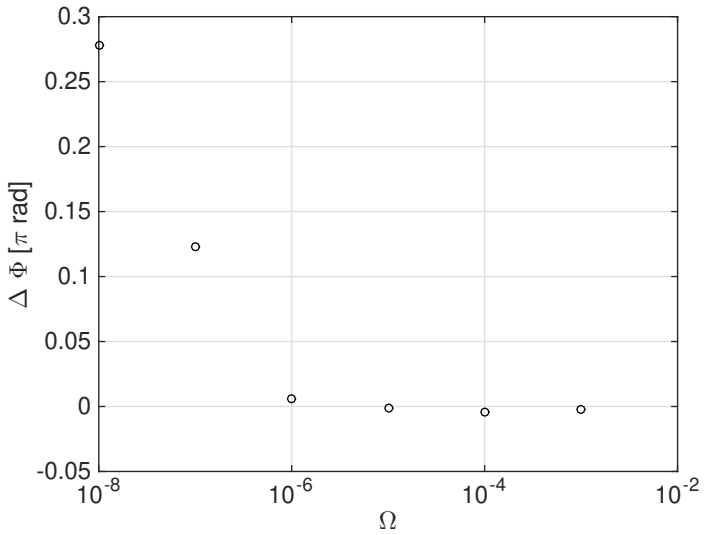

FIG. 9: Phase shift $\Delta\Phi$ as a function of Ω.

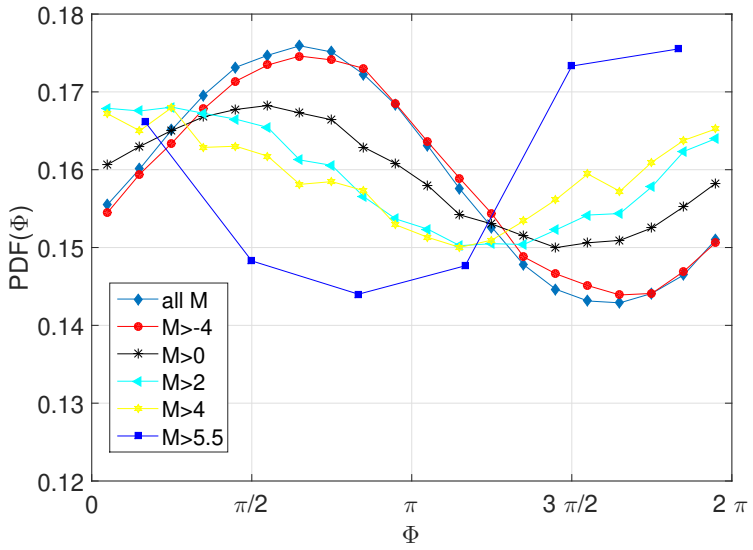

FIG. 10: PDF of the phase Φ for $\Omega = 10^{-7}$ and $\varepsilon = 10^{-2}$ and for events of magnitude larger than M_s, see legend for the value of M_s.

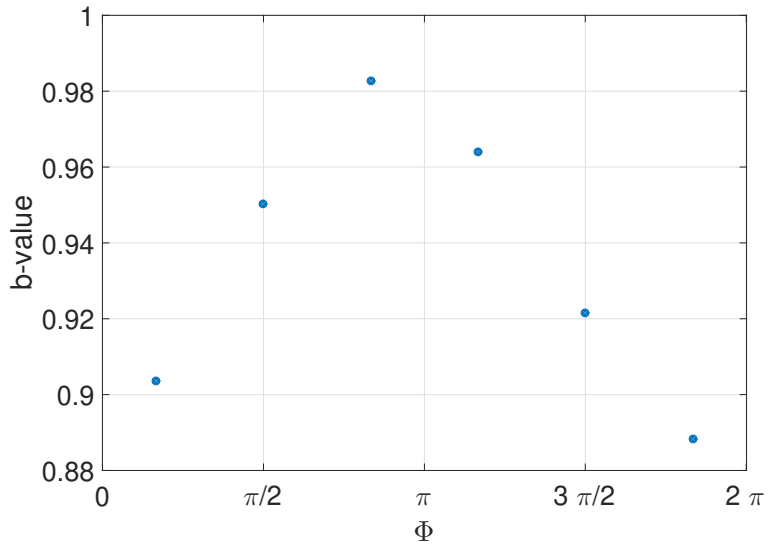

FIG. 11: b-value calculated by a fit for $0.5 \leq M \leq 3$ for events with phase Φ restricted to $[k, k+1[\pi/3$. Same data as in fig 10

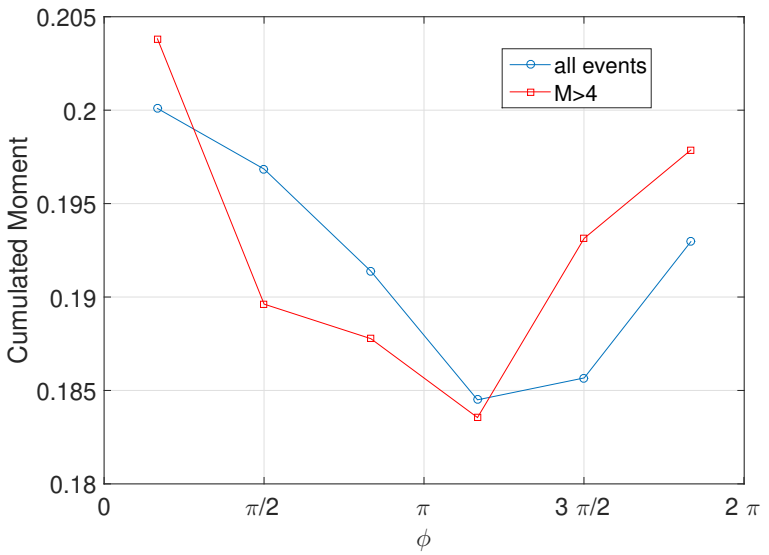

FIG. 12: Distribution of the cumulated moment for events with phase Φ restricted to $[k, k+1[\pi/3$, for $\Omega = 10^{-7}$ and $\varepsilon = 10^{-2}$. Blue: all events, red $M > 4$.

Results

No modulation

Numerical simulations of the model have shown that for α smaller than $1/4$, the dynamics generates events of magnitude that is widely distributed. More precisely a G-R law is observed with a b-value that varies with α [25, 29].

We have focused on two values of α, 0.15 and 0.225. We consider a system of size 30^2 close to the $N = 800$ masses that we studied in the BK model. We set $v_0 = 10^{-6}$ and vary ε and Ω.

Modulated normal stress model (NSM)

Most results are similar to the ones observed in the BK model. For moderate ε, the GR law is not modified but events occur preferentially for certain values of the phase, $\Phi = \Omega T$ modulo 2π. Then, the distribution of the phase, $PDF(\Phi)$ is a harmonic function that we fit to obtain the amplitude of the response a and the phase-lag with respect to the forcing.

We display in figure 13 the value of the response a as a function of ε.

We define ε_c, the value of ε at which a reaches $10^{-2}\sqrt{2}$. It is displayed in fig. 14. Two regimes are observed: at large Ω, ε_c is proportional to Ω^{-1} and it saturates at small Ω.

At moderate ε, smaller than a few times ε_c, the response of the system is linear in ε. The results for a as a function of $\varepsilon/\varepsilon_c$ are collapsed on a master curve displayed in fig. 15.

The phase-lag between the modulation and the response is displayed in fig. 16. At large Ω, events occur preferentially when the decay rate of F_0 is the largest. Decreasing Ω, the system has a tendency to generate more events when the friction force is the smallest.

We have also studied how the phase distribution is dependent on magnitude M. We consider ε close to ε_c and have varied Ω and α. We have observed that for large enough Ω the distribution of the phase is not dependent on M. In contrast, for smaller Ω the distribution changes with M.

The global behavior is similar to the one of the BK model, larger magnitudes have a distribution peaked at a phase for which the friction force is the largest, while smallest events are more likely when the friction force is the smallest. In terms of the magnitude distribution, this amounts to a variation of the b-value as a function of phase, see fig. 18.

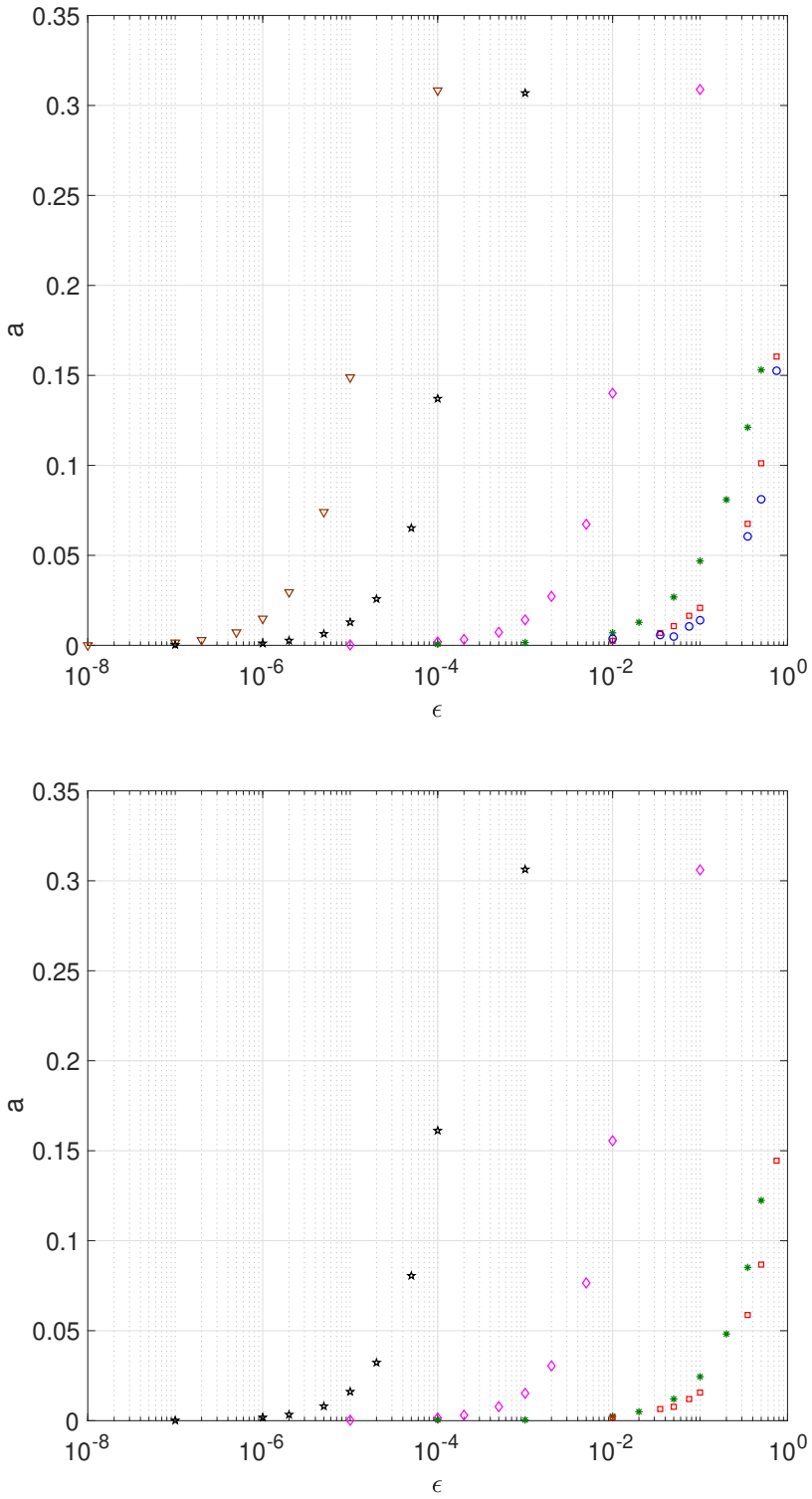

FIG. 13: Amplitude of the modulation of the phase distribution a as a function of ε for top: $\alpha = 0.15$ and Ω: ($\circ$ blue) 10^{-8}, ($\square$ red) 10^{-7}, ($\star$ green) 10^{-6}, ($\diamond$ magenta) 10^{-4}, ($\star$ black) 10^{-2}, ($\triangle$ marron) 10^{-1}; bottom: $\alpha = 0.225$ and Ω: ($\square$ red) 10^{-7}, ($\star$ green) 10^{-6}, ($\diamond$ magenta) 10^{-4}, ($\star$ black) 10^{-2}.

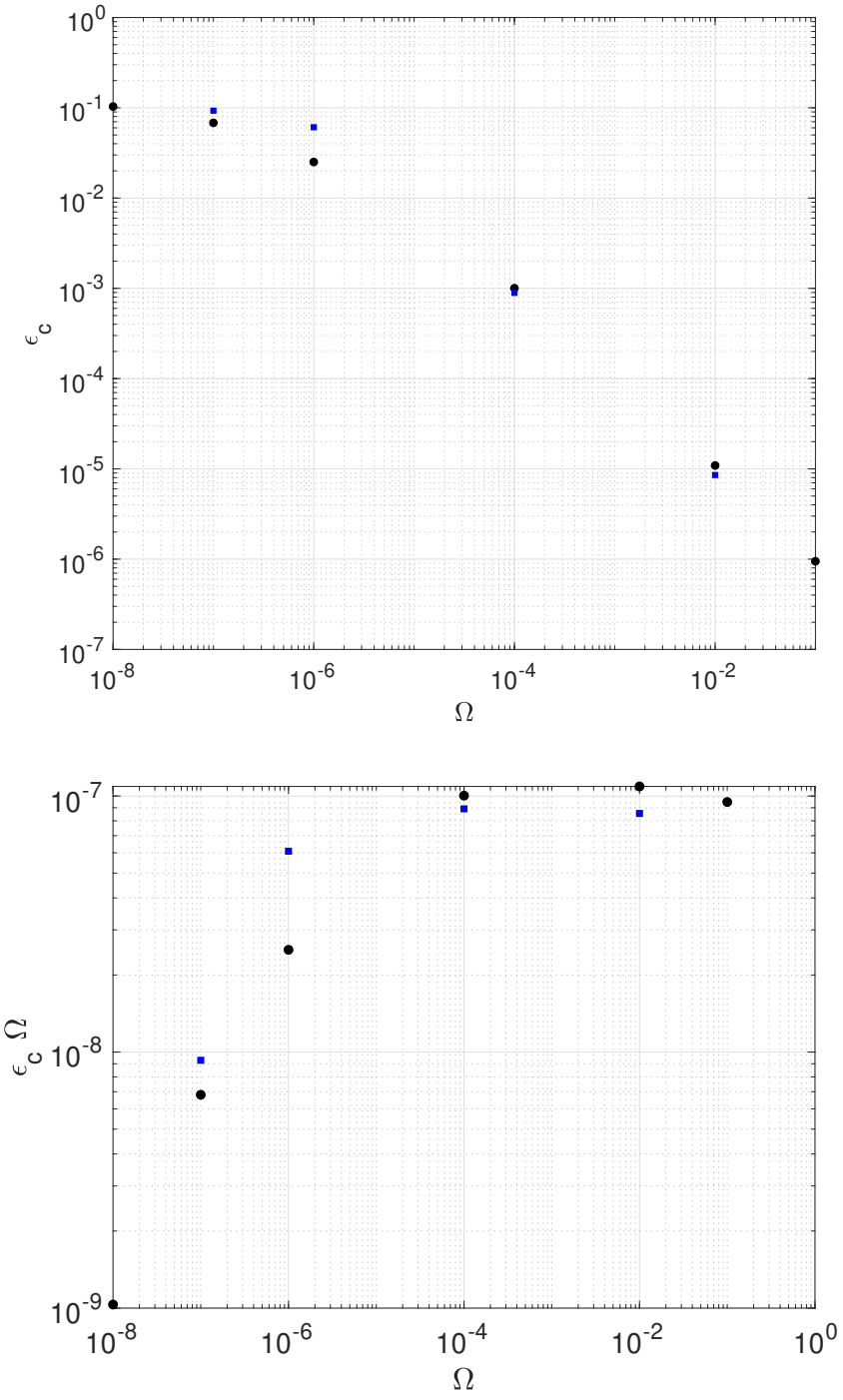

FIG. 14: Top: ε_c as a function of Ω. Bottom: $\Omega\varepsilon_c$ as a function of Ω. Symbols stand for the values of α. (•): $\alpha = 0.15$, (□): $\alpha = 0.225$.

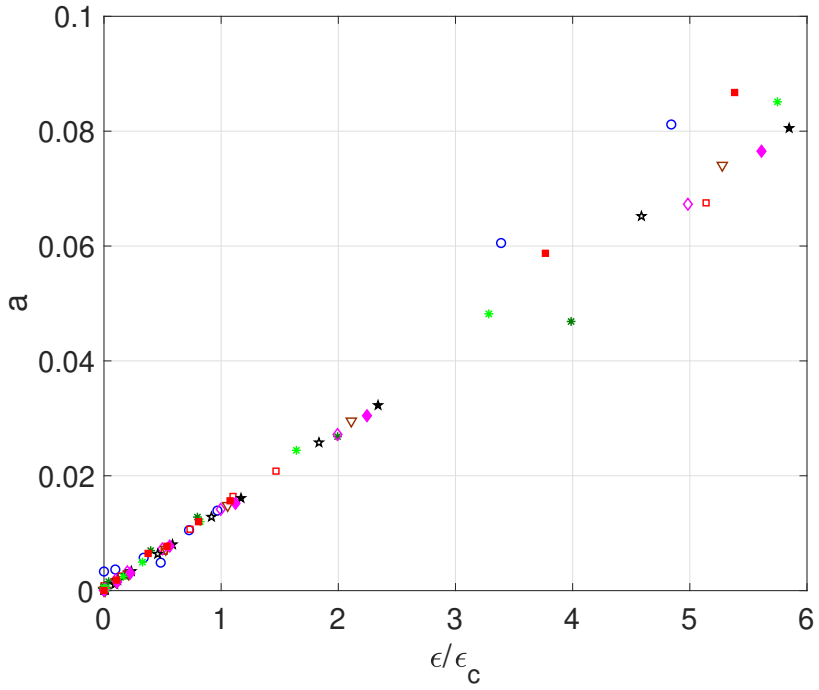

FIG. 15: Amplitude of the modulation of the phase distribution a as a function of $\varepsilon/\varepsilon_c$ for different frequencies and $\alpha = 0.225$ (full symbols) and $\alpha = 0.15$ (empty symbols). The values of Ω are the same as in fig. 14.

Modulated shear stress model (SSM)

We observe behaviors similar to the case of modulated normal stress with the only exception that the distribution of the phase do not depend on magnitude.

DISCUSSION

Mechanisms responsible for the observed behaviors

Several properties due to a modulation of the normal stress or of the shear stress are observed in both the one dimensional BK and the two dimensional OFC model. These properties are thus likely to be generic and we now discuss their possible origin.

We first analyze the origin of the modulation of $P[\phi]$, in the case of a modulation of the normal stress unless otherwise stated.

For Ω larger than Ω_c, the modulation favors the occurrence of EQ when the decreasing rate of

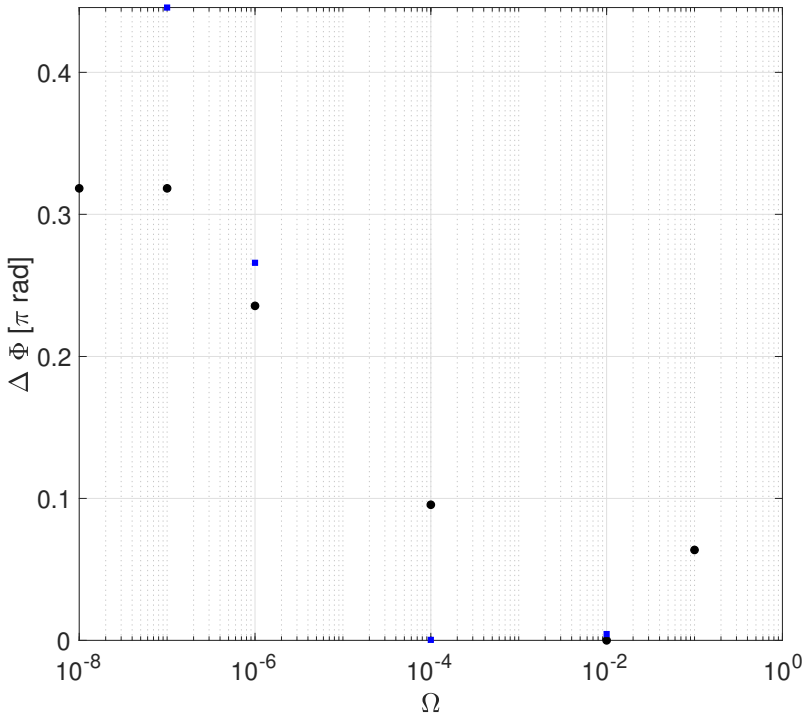

FIG. 16: Phase shift $\Delta\Phi$ as a function of Ω for ($\bullet$): $\alpha = 0.15$, ($\square$): $\alpha = 0.225$.

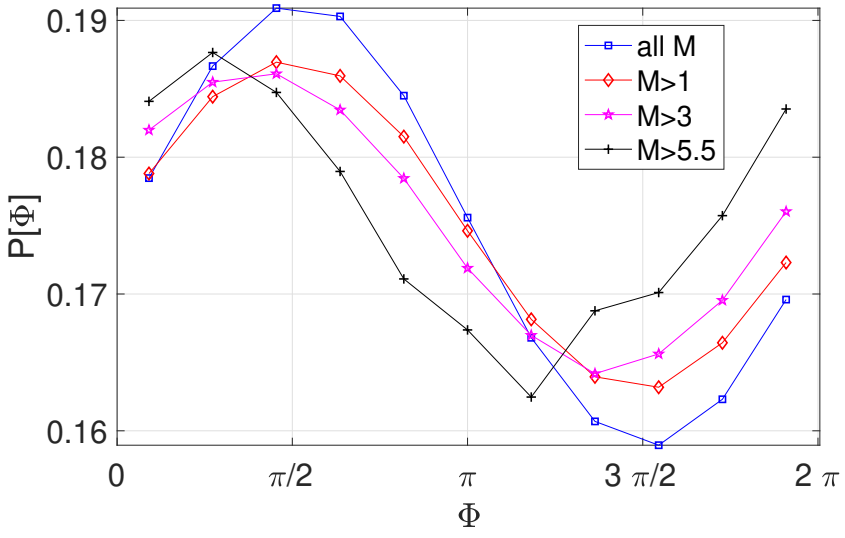

FIG. 17: PDF of the phase Φ for $v_0 = 10^{-8}$, for $\alpha = 0.225$, $\varepsilon = 10^{-2}$ and $\Omega = 10^{-7}$ and for events of magnitude larger than M_s, see legend for the value of M_s.

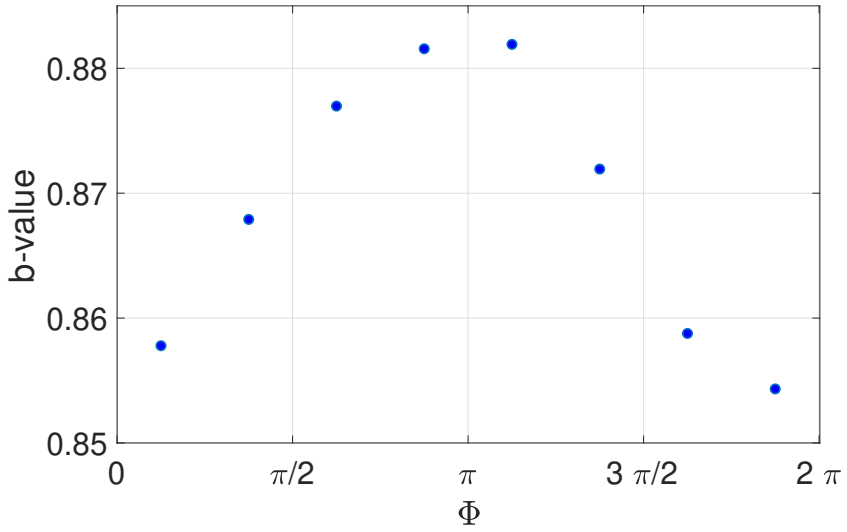

FIG. 18: b-value calculated by a fit for $2.3 \leq M \leq 4.5$ for events with phase Φ restricted to $[k, k+1[\pi/4$. Same data as in fig 17.

the normal stress is the largest. This results from the criterion to initiate an EQ: an event starts when the loading force reaches the static friction. If the latter increases with time, it is more difficult for the driving force to initiate an EQ, see illustration in fig. 19. This behavior does not depend on the EQ magnitude. For the case of a modulated shear stress, we observe a similar behavior, in which events occur when the increasing rate of the shear stress is the largest.

We can understand this regime quantitatively as follows. Driving of the upper plate leads to the constant stressing rate of v_o for each block. An event occurs at the moment when the shear stress exceeds the static friction stress. In the case of normal stress modulation, the static friction depends on time as $1+\varepsilon\cos(\Omega t)$. Let Σ_{i-1} be the difference between the residual stress and the friction force after the $i-1$-th event that took place at time t_{i-1}. The time t_i at which the total stress reaches the static friction again is given by the solution of

$$v_0(t_i - t_{i-1}) + \Sigma_{i-1} = 1 + \varepsilon\cos(\Omega t_i), \tag{7}$$

We note that this equation allows for multiple solutions if ε is large. Hereafter we assume sufficiently small ε so that there exists a single solution for t_i. Let us define the phase $\Phi_i = \Omega t_i$, we have

$$\Phi_i - \frac{\varepsilon\Omega}{v_0}\cos(\Phi_i) = \Phi_{i-1} + \Omega\frac{1-\Sigma_{i-1}}{v_0}. \tag{8}$$

We note θ_0 the right hand side and observe that it contains the term Σ_{i-1} which value is set by

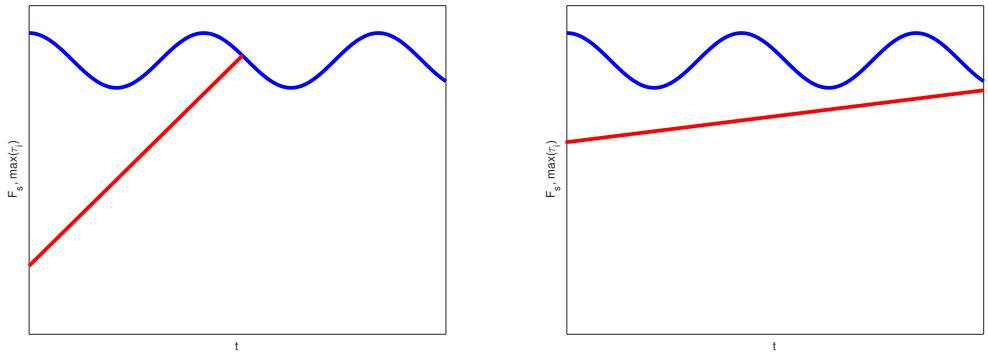

FIG. 19: Sketch of a loading phase. For a modulated friction force (NSM): the maximum load, $max(\tau_i)$, increases linearly in time. The static friction force, F_s, is periodically modulated. An EQ starts when the two forces are equal. Left: the modulation rate is comparable to the linear loading rate. The condition for EQ occurence is more easily satisfied when the friction force decay rate is the largest. In the case of a modulated shear stress (SSM), the same discussion is valid taking into account that the linear-in-time increasing load contains only the term of constant shear rate whereas the oscillating term is equal to the static friction force minus the modulated part of the shear stress.
Right: In the case of a very large modulation rate, the linear load appears nearly horizontal. Events occur only at the minimum of the oscillating curve, thus when the friction force is the smallest.

the dynamics during the preceding EQ and varies with the event number i. We can express the probability of Φ_i from the one of θ_0 as

$$P[\Phi] = P[\theta_0]\frac{d\theta_0}{d\Phi}, \tag{9}$$

and use from equation 8 that $d\Phi\,(1+\frac{\varepsilon\Omega}{v_0}\sin(\Phi)) = d\,\theta_0$, so that

$$P[\Phi] = P[\theta_0]\,(1+\frac{\varepsilon\Omega}{v_0}\sin(\Phi))\,. \tag{10}$$

When the variations of $P[\theta_0]$ are small so that it can be considered as a constant, this equation predicts the form of $P[\Phi]$ observed at large Ω : $\Delta\Phi = 0$ and a coefficient a proportional to ε. Using the normalization of the PDF, we even obtain $h = av_0/(\varepsilon\Omega) = (2\pi)^{-1} \simeq 0.159$ in perfect agreement with the values measured at large Ω and $\alpha \leq 1$.

For Ω smaller than Ω_c, events are more frequent when the friction force is the smallest. This can also be understood from the criterion that controls the initiation of an event, see fig. 19. We

note that at small Ω, the amplitude of force modulation ε required to observe a modulation of the phase of the event is large. This is the not the case in the large Ω regime because then the modulation of the phase takes place for very small values of ε as it results from a competition between the load speed v_0 and the speed of change of the friction force $\varepsilon\Omega$.

The behavior for small Ω is due to events of small magnitude that dominate the statistics if we consider all events. If we consider only events above a magnitude M_s, the behavior changes with M_s. In particular, for the largest magnitudes, events occur preferentially when the normal force is the largest. For such rare events, the largest the friction force, the strongest is the load when the event is initiated so that more energy is available to be transferred to the motion of the blocks.

For the case of a modulation of the shear stress, the regime of small Ω is different and in particular does not depend on the magnitude of the events. This indicates that the sensitivity of the effects of the modulation on the frequency or on the event magnitude is controlled by the dynamics during the phases where the blocks are moving. More precisely, in the SSM for the BK model, if we write the dynamical equations with x_i, x_{i-1}, x_{i+1} and their values at the beginning of the event, the modulated term ($\varepsilon \cos \Omega t$) does not appear in the equation and thus has no effect on the dynamics. Similarly, for the OFC model, the modulation only affects the loading phase. In contrast, in the NSM model, the modulation favors the motion for phase $\phi \simeq 0$ and inhibits it for phases close to π. This results in an increase in the number of small events for $\phi \simeq \pi$ when the normal stress is minimum, and an increase in the number of large events for $\phi \simeq 0$ when the normal stress is maximum.

In the case where both the normal and the shear stress are modulated, a sensitivity to magnitude is expected. The larger the normal stress modulation, the larger the sensitivity. More precisely, the effect is large provided the modulated term has a noticeable effect during the dynamical phases: reducing the acceleration for some values of the phase and enhancing it for other values.

Orders of magnitude for real earthquakes

To connect with observations performed on natural earthquakes, we need to use dimensional quantities. The amplitude of the triggering effect for the moderate stress modulation can be written

$$a \propto \frac{\hat{F}\varepsilon\hat{\Omega}}{\hat{v_0}\hat{k}_1}. \tag{11}$$

We can then define the susceptibility of EQs to stress modulation as

$$\chi \equiv \frac{\partial a}{\partial(\varepsilon \hat{F})} \propto \frac{\hat{\Omega}}{\hat{v_0}\hat{k}_1}. \tag{12}$$

The dimension of χ is the inverse of stress, and $1/\chi$ is regarded as the characteristic stress, at which the response of the phase distribution to stress modulation is of the order of unity. A stress perturbation of $0.1/\chi$ is thus sufficient to cause a significant correlation of EQs with stress modulation. The denominator $\hat{v_0}\hat{k}_1$ in Eq. (12) is the stressing rate to the sliders, and therefore the ratio of the modulation frequency to the stressing rate controls the sensitivity of EQs to stress modulation.

Then we can compare our model with the natural EQs based on Eq. (12). The stressing rates in natural earthquake faults and tectonic plate boundaries may be $\dot{\gamma}G$, where $\dot{\gamma}$ is the strain rate and G is the shear modulus of the Earth's crust. While $G \simeq 30$ GPa [31], the strain rate at tectonic plate boundaries may vary by orders of magnitude. Here we adopt $\dot{\gamma} \simeq 10^{-15}$ to 10^{-12} s^{-1} [26]. These values give the stressing rate of 3×10^{-5} to 3×10^{-2} [Pa/s]. The period of stress modulation $2\pi/\hat{\Omega}$ ranges from half a day ($\hat{\Omega} \simeq 1.5 \times 10^{-4} s^{-1}$) to nearly one month ($\hat{\Omega} \simeq 2.5 \times 10^{-6} s^{-1}$) for tides, while it may be half a year for seasonal loading ($\hat{\Omega} \simeq 2 \times 10^{-7} s^{-1}$). Then the susceptibility may range from 6.7×10^{-6} to 5.0 [1/Pa], which corresponds to the characteristic stress of 0.2 to 1.5×10^5 [Pa]. The range is too broad to allow any quantitative comparison with the observation data, but at least does not contradict to the typical stress modulation observed on the Earth: 10^3 to 10^4 [Pa] for tidal [3] and seasonal loading [35].

Magnitude sensitivity occurs in the case of low frequency modulation. Then, the crossover frequency Ω_c is of the order of 10^{-6}, which can be expressed as $\hat{\Omega}_c \simeq 100\hat{v_0}\hat{k}_1/\hat{F}$. We note that $\hat{F}/\hat{v_0}\hat{k}_1$ may be regarded as the the recurrence time of earthquakes at a given location, *i.e.* the time interval between two sufficiently large events at a given place. With this definition, the crossover time $T_c = 2\pi/\hat{\Omega}_c$ is roughly ten times smaller than the recurrence time of earthquakes. Namely, if the period of normal stress modulation is comparable to the recurrence time of earthquake, it can affect the b-value and the magnitude of EQs. This is the case of earthquakes with recurrence time of the order of a few years subject to seasonal loading. In some sense, this mechanism also provides a possible explanation for the change in the b-value observed during the evolution of a fault between two very large events throughout the earthquake cycle [37]. Long term evolution of the normal stress would then be due to tectonic motion and not to tidal or seasonal modulations.

Possible limitations

In the two models, it appears clearly that a large modulation of the stress rate results in strong correlations between stress rate and phase of the events. Yet, such correlations are not always reported.

A possible explanation for this disagreement lies in the absence of nucleation process in both models. As pointed out in [2], stress variations that would occur on time scales shorter than the nucleation time are expected to be inefficient at triggering earthquakes.

The absence of nucleation process in our models plays also a role for comparing with other models. The rate and state model of [33], see also [34], predict behaviors that depend on whether the modulation period is large or small compared to the nucleation time. At small period, an increased activity is predicted when the stress is large, whereas at large period, activity is large when the stress rate is large. The behavior in our models also depend on the modulation frequency. For instance for the NSM model, by increasing the modulation time, the response changes from a correlation with stress rate to a correlation with stress amplitude. The crossover period is a fraction of the recurrence time of the fault. We note that nucleation processes are absent in our models so that this can explain the absence of a sensitivity to stress amplitude at smallest modulation period as predicted in the rate and stress models. A possible scenario that would reconcile these models is that at period shorter than then nucleation time, a sensitivity (probably small) to stress amplitude takes place, at intermediate period, a stronger sensitivity to stress rate occurs, and at period larger than a fraction of the recurrence time of the fault a correlation with stress amplitude is recovered.

Another effect that is not taken into account in our model is the perturbation due to distant earthquakes. Such earthquakes act on a given fault as a source of noise due to the random emission of seismic waves. These waves can trigger earthquakes even at distance, and may thus mask the effect of tides.

An important result of this study is the possibility for a magnitude dependence of the properties. Magnitude dependence of seasonality of deep earthquakes have been discussed in [9]. For what concerns tidal effects, [13] reports that very large earthquakes occur near the time of maximal tidal stress whereas this tendency is not obvious for small earthquakes. In the model that displays magnitude sensitivity (NSM model for a small modulation frequency), we stress that the observed behaviors are not straightforward: for the parameters of fig. 10, events with largest amplitude occur more often when the normal force is the largest, very small events are more likely to occur when

the normal force is the smallest and events of intermediate amplitude have a smaller sensitivity to the modulation. We note that in natural data, the latter could easily be considered as not statistically significant and would thus correspond to the small earthquakes reported in [9]. The smallest events of the model would then either be undetected in natural data or inexistant.

Again, it is important to discuss why variations of the behavior with magnitude might be absent in natural datas. The limitations mentionned earlier and due to the absence of nucleation process and of dynamical triggering by distant earthquakes could be the cause. In addition, for the models considered here, only a modulation of the normal stress results in magnitude dependence of the correlation between modulation and EQ occurrences. In more general settings, both the normal and the shear stresses are modulated. Then the larger the normal stress modulation, the larger the sensitivity to magnitude. One of such tectonic settings is the subduction zone with a low dip angle. In contrast for faults subject predominantly to shear stress modulation, no magnitude dependence is expected.

Finally, considering a single harmonic component to model tidal forcing is obviously oversimplified. More realistic models are needed but it is satisfying that with such a simple hypothesis, a variety of predictions can be made and compared to natural observations.

Prospects

From the point of view of statistical physics, this work is a study of the susceptibility of out-of-equilibrium systems in the vicinity of a scale invariant regime. More precisely, the susceptibility may be written as $\chi(k,\Omega)$ with k being the wavenumber. Then Eq. (12) corresponds to this susceptibility at zero wavenumber $k=0$ and we have studied its dependence on Ω here. Investigating the effect of a finite wavenumber would be of interest and might define characteristic lengths of the system. At $k=0$, we identified a crossover frequency Ω_c below which the linear susceptibility changes behavior. In particular for a modulated normal stress, the susceptibility becomes magnitude dependent. It would be of interest to investigate similar properties in other scale invariant systems, even at equilibrium. Here, the fact that the magnitude dependence is not observed with a modulated shear stress indicates that the two models do not belong to the same universality class, even though the differences between them are apparently minor.

Following theoretical works could consider different friction laws (such as the R & S friction

law) and more realistic modulations. In particular, a modulation made of two frequencies would be a better model of tidal forcing when the different tidal components are of comparable amplitudes. For large modulation frequencies and as in the present study, we expect an increase of the number of events during the phases where the decay rate of the friction force is the largest. The behavior at small modulation frequency and its possible magnitude dependence is also likely to lead to interesting effects.

We did not identify clear change in the susceptibility in the vicinity of a large earthquake. In the BK model without modulation, there already exists a clear decay in activity between before and after a large EQ. This (unrealistic) property dominates the changes of behavior. More realistic models would be useful to reveal possibly small variations in the susceptibility as an indicator of mainschock.

From the point of view of data analysis, our results show that the behavior of the system depends on several parameters. First, whether the normal or the shear stress are modulated, thus on the type of fault and of loading. Second, on the ratio between the modulation time and the inter-event time. Catalogs should be analyzed taking into account these parameters. It would also be interesting to investigate whether some faults display quiescence, *i.e.* total absence of events during some phases of the modulation, which is the most extreme regime identified in this study.

Acknowledgements

We thank the PHC Sakura 38585WH for his support. This study was initiated following visits to ERI by AS and FP and a visit to the Department of Geosciences by TH. FP, AS and TH gratefully acknowledge the visiting scientists programs of both institutions. AS gratefully acknowledges the support of the European Research Council grant REALISM (2016-grant 681346). TH and TS are also supported by the MEXT under "Exploratory Challenge on Post-K computer" (Frontiers of Basic Science: Challenging the Limits). TH gratefully acknowledges additional support from JSPS KAKENHI Grant JP16H06478.

[1] A. Schuster, Proc. R. Soc. London, 61, 455-465, 1897.

[2] Dieterich, J. H., Tectonophysics 211.1-4 (1992): 115-134.

[3] Beeler, N. M., and D. A. Lockner., Journal of Geophysical Research: Solid Earth 108.B8 (2003).

[4] Metivier, Laurent, et al., Earth and Planetary Science Letters 278.3-4 (2009): 370-375.

[5] Thomas, A. M., et al. "Tidal triggering of low frequency earthquakes near Parkfield, California: Implications for fault mechanics within the brittle-ductile transition." Journal of Geophysical Research: Solid Earth 117.B5 (2012).

[6] S. Ide and Y. Tanaka, GRL 41, 3842-3850, 2014.

[7] Cochran, E.S., Vidale, J.E. and Tanaka, S. Earth tides can trigger shallow thrust fault earthquakes, Science, **306**, 1164–1166 (2004).

[8] Hill, David P. "Dynamic triggering." Treatise on geophysics (2007): 257-292.

[9] S. Ide, S. Yabe and Y. Tanaka, Nature Geoscience (9), 834-838, 2016.

[10] S. Tanaka, M. Ohtake and H. Sato, Journal of Geophysical Research, 107, 2211, 2002.

[11] S. Tanaka, GRL 39, L00G26, 2012.

[12] S. Tanaka, GRL 37, L02301, 2010.

[13] Z. Zhan and P. M. Shearer, GRL 42, 7366-7373, 2015.

[14] L. Bollinger et al., GRL 34, L08304, (2007).

[15] Ader, T.J., and Avouac, J.-P. Detecting periodicities and declustering in earthquake catalogs using the Schuster spectrum, application to Himalayan seismicity, Earth and Planetary Science Letters, **377-378**, 97-105 (2013).

[16] Christiansen, L.B., Hurwitz, S., and Ingebritsen, S.E. Annual modulation of seismicity along the San Andreas Fault near Parkfield, CA. Geophysical Research Letters, **34**, L04306 (2007).

[17] Johnson C.W., Fu, Y., and Bürgmann, R. Seasonal water storage, stress modulation, and California seismicity, Science, **356**, 1161-1164 (2017).

[18] Craig, T. J., Chanard, K., and Calais, E.. Hydrologically-driven crustal stresses and seismicity in the New Madrid Seismic Zone, Nature communications, 8 (1), 2143 (2017).

[19] Ueda T., Kato A., Seasonal variations in crustal seismicity in the San-in district, Southwest Japan, Geophysical Research Letters **46** L081789 (2019).

[20] T. J.. Ader, J.-P. Ampuero and J.-P. Avouac, Geophysical Research Letters, **39** L16310 (2012)

[21] T.J. Ader et al, Geophys. J. Int. **198**, 385–413, (2014) .

[22] For completeness of the dimensional analysis, the slider masses are equal to $\hat{m}$. The friction force are $\hat{m}\hat{F}$ so that after dividing the dynamical equation by $\hat{m}$; it disappears of the equations and of the dimensional analysis.

[23] Some authors introduce $l = \sqrt{K}$ and here $l = 3$.

[24] More precisely, for ε larger than roughly $10 - 15\varepsilon_c$, see definition of ε_c later on.

[25] H. Kawamura et al., Rev. Mod. Phys. 84, 839, (2012).

[26] Kreemer Corn, Geoffrey Blewitt and Elliot C. Klein, Geochemistry, Geophysics, Geosystems, 15.10, 3840-3889 (2014).

[27] Kanamori, Hiroo, and Emily E. Brodsky. "The physics of earthquakes." Reports on Progress in Physics 67.8 (2004): 1429.

[28] Ito, Yoshihiro, et al. "Slow earthquakes coincident with episodic tremors and slow slip events." Science 315.5811 (2007): 503-506.

[29] Z. Olami, H. J. S. Feder and K. Christensen, Physical Review Letters, **68**, 1244-1248 (1992).

[30] A. Helmstetter, S. Hergarten and D. Sornette, Physical Review E, **70**, 046120 (2004).

[31] Jaeger, John Conrad, Neville GW Cook, and Robert Zimmerman. Fundamentals of rock mechanics. John Wiley & Sons, 2009.

[32] We obtain $h = av_0/(\varepsilon\Omega) = 0.16$ for $\Omega = 10^{-3}$ and $av_0/(\varepsilon\Omega) = 0.17$ for $\Omega = 10^{-7}$.

[33] J. Dieterich, "A constitutive law for rate of earthquake production and its application to earthquake clustering", J. Geophys. Res. Solid Earth, 99 (B2), 2601—2618 (1994).

[34] Heimisson , E. R, and Jean-Philippe Avouac, Analytical prediction of seismicity rate due to tides and other oscillating stresses, submitted to GRL, EarthArXiv (2020). Heimisson, E. R., and Segall, P. "Constitutive law for earthquake production based on rate-and-state friction: Dieterich 1994 revisited", Journal of Geophysical Research: Solid Earth, 123(5), 4141—4156, (2018).

[35] van Dam, Tonie, et al. "Crustal displacements due to continental water loading." Geophysical Research Letters 28.4 (2001): 651-654.

[36] Ide, Satoshi. "The proportionality between relative plate velocity and seismicity in subduction zones." Nature Geoscience 6.9 (2013): 780.

[37] Nanjo, K. Z., Hirata, N., Obara, K., and Kasahara, K., "Decade-scale decrease in b value prior to the M9-class 2011 Tohoku and 2004 Sumatra quakes", Geophysical Research Letters, 39 (20), 20304 (2012).